# Supporting Information

## Porous organic polymers with spiro-thioketal linkages for effective iodine capture

Wen-Jun Lu, Yu-Heng Ma and Bai-Wang Sun*

School of Chemistry and Chemical Engineering, Southeast University,

Nanjing, 211189, P. R. China

*E-mail: chmsunbw@seu.edu.cn

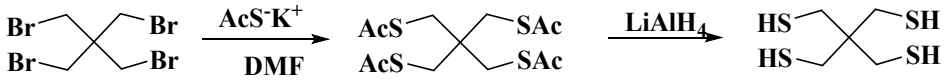


TSAc TSH

**Synthesis of tetrathiapentaerythritol (TSH)**

Pentaerythrityl tetrathioacetate (TSAc) was synthesized following the methodology described in the previous literature. [S1] In a 500 mL reaction flask, 3.88 g of pentaerythrityl tetrabromide (10 mmol) and 9.12 g of potassium thioacetate (80 mmol) were added. Subsequently, 150 mL DMF was introduced into the flask. Then the mixture was stirred at 25 °C for 3 days. The brown mixture was added into 1 L water, then the product was filtered, which was further purified by recrystallization from methanol to yield TSAc (2.40 g, 65.2%). $^1$H NMR (400 MHz, Chloroform-d) δ 3.05 (s, 8H), 2.37 (s, 12H). $^1$H NMR spectrum was shown in Fig. S1.

Tetrathiapentaerythritol (TSH) was obtained by a modified procedure described by Yang for synthesis of SH groups. [S2] To a suspension of $LiAlH_4$ (100 mmol, 3.8 g) in 100 mL dry THF cooled with an ice bath, a solution of pentaerythrityl tetrathioacetate (9.185 mmol, 3.38 g) in 75 mL dry THF was added. The reaction mixture was stirred under nitrogen atmosphere and the completion of the reaction was monitored by TLC. Water was carefully added in order to neutralize the excess of $LiAlH_4$, then the entire mixture was quenched in concentrated HCl (12 M) and stirred until a clear solution was obtained (pH = 1). The mixture was extracted three times with dichloromethane (3×80 mL). The separated organic phase was dried over $Na_2SO_4$ and the solvent was then removed under reduced pressure. The crude product was crystallized from ethanol to give white crystal (yield: 1.49 g, 81%). $^1$H NMR (400 MHz, Chloroform-d) δ 2.66 (d, J = 8.8 Hz, 8H), 1.24 (t, J = 8.7 Hz, 4H). $^1$H NMR spectrum was shown in Fig. S2.

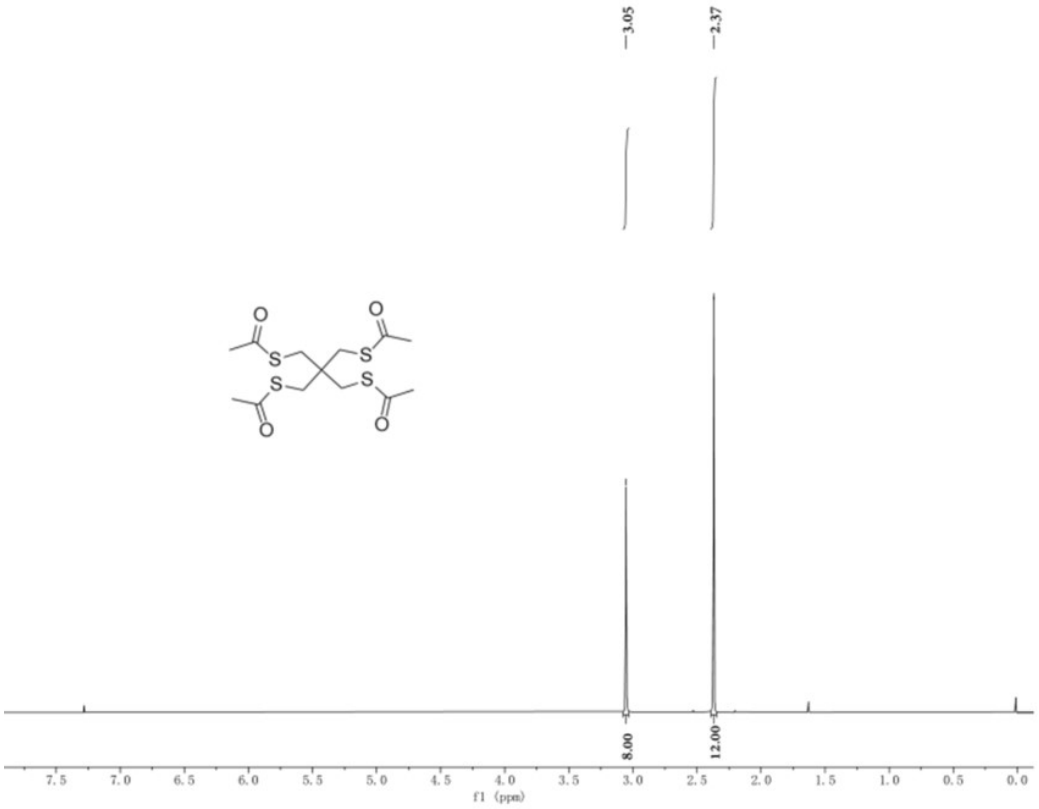


Fig. S1. $^{1}$H NMR spectrum of TSAc.

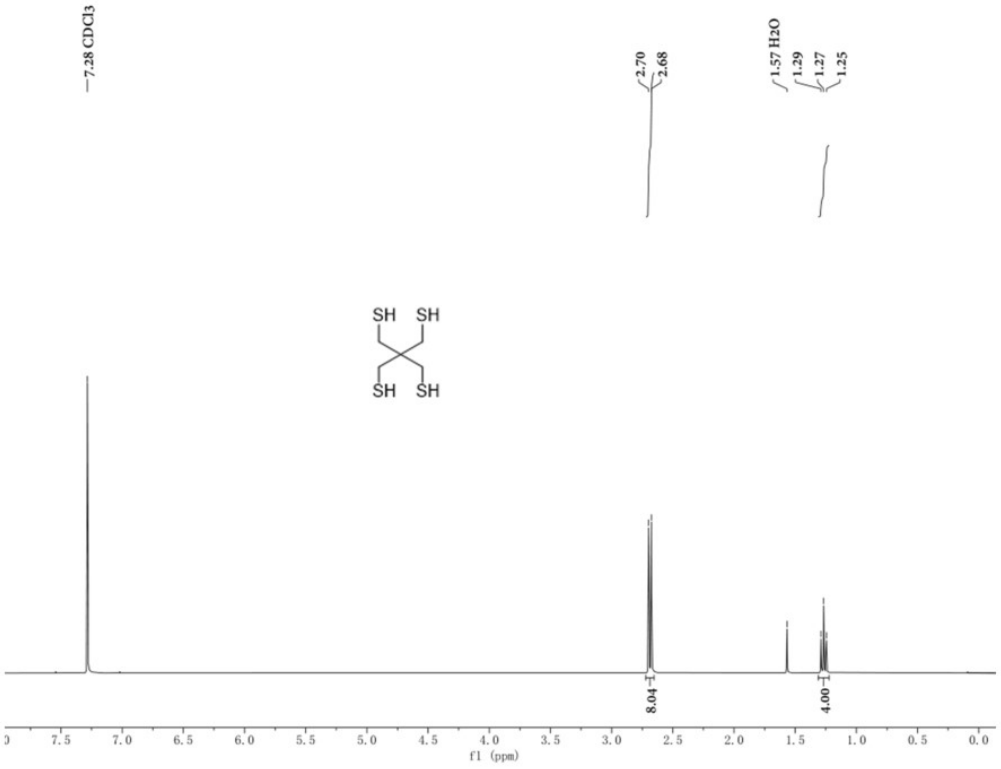


Fig. S2. $^{1}$H NMR spectrum of TSH.

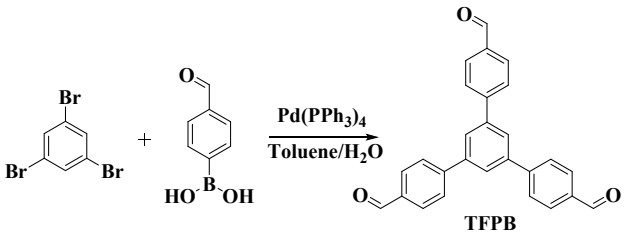


**Synthesis of 1,3,5-tris(4-formylphenyl)benzene (TFPB)**

**TFPB** was synthesized according to a modified method. [S3] A mixture of 4-formylphenylboronic acid (2.43 g, 16.2 mmol), 1,3,5-tribromobenzene (0.85 g, 2.7 mmol), $Pd(PPh_3)_4$ (289 mg, 0.25 mmol), potassium carbonate (2.76 g, 20 mmol), 1,4-dioxane (40 mL), and distilled water (10 mL) was stirred at 90 °C under $N_2$ atmosphere for 24 h. After cooled at room temperature, the precipitate was collected by filtration and the residue was purified by flash column chromatography (petroleum ether/ethyl acetate (10:1); silica gel: 200-300 mesh) to give TPB as a white solid in 81.6% yield (0.86 g, 2.2 mmol). $^1$H NMR (400 MHz, Chloroform-*d*) δ 10.13 (s, 3H), 8.08-8.02 (m, 6H), 7.94 (s, 3H), 7.92-7.88 (m, 6H). $^{13}$C NMR (101 MHz, $CDCl_3$) δ 191.76, 146.30, 141.60, 135.77, 130.44, 127.98, 126.48, 126.41. $^1$H NMR and $^{13}$C NMR spectrum was shown in Fig. S3 and Fig. S4.

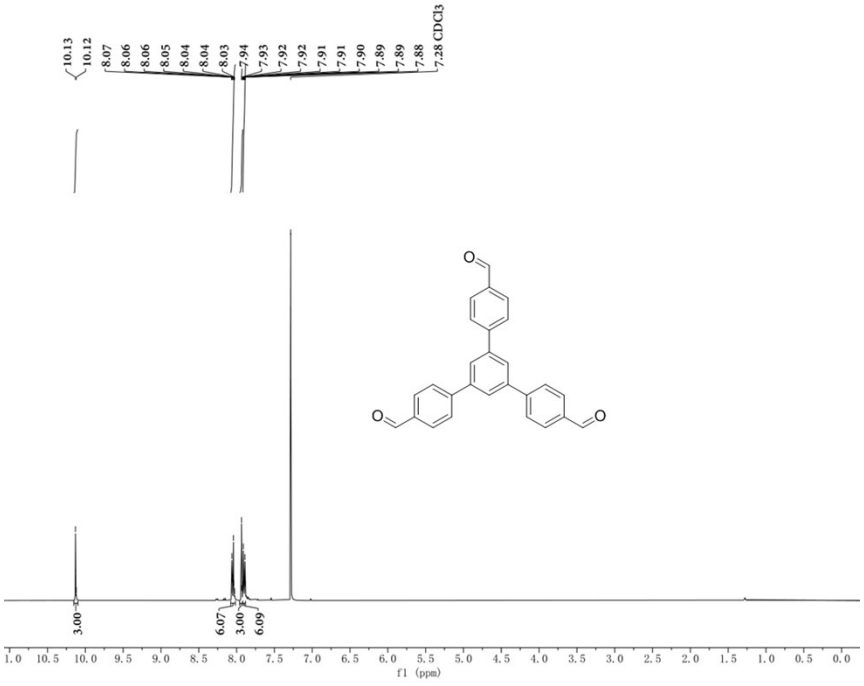


Fig. S3. $^1$H NMR spectrum of **TFPB**.

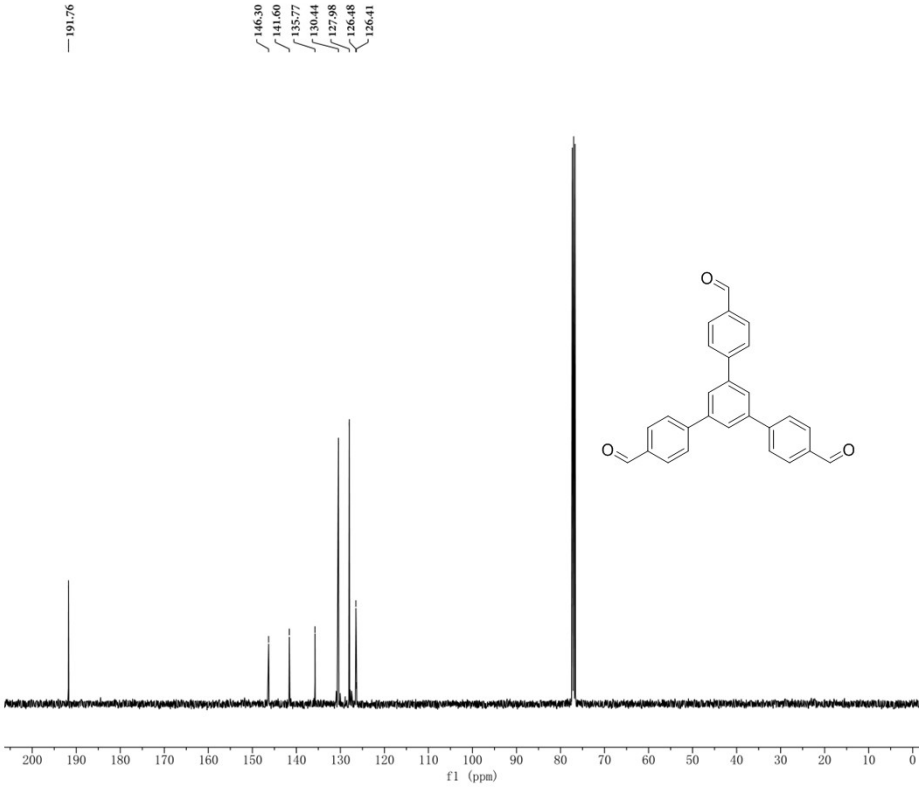


Fig. S4. $^{13}C$ NMR spectrum of **TFPB**.

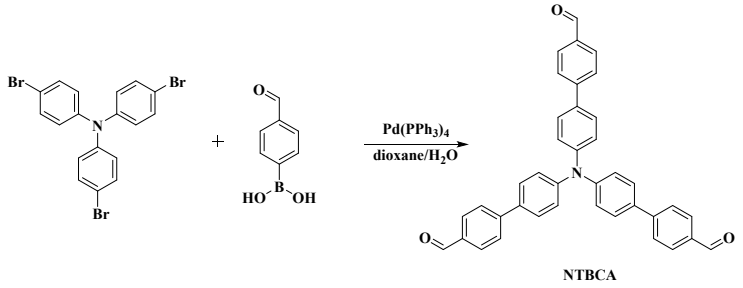


**Synthesis of 4',4''',4''''''-nitrilotris(([1,1'-biphenyl]-4-carbaldehyde)) (NTBCA)** [S4]

Tris(4-bromophenyl)amine (2.41 g, 5 mmol) and 4-formylphenylboronic acid (3 g, 20 mmol) were dissolved in 80 mL dioxane. Aqueous solution of $K_2CO_3$ (5.5 g, 40 mmol) was added into the dioxane solution under $N_2$ atmosphere. After the addition of $Pd(PPh_3)_4$ (300 mg 0.26 mmol) to the degassed mixed solution with vigorous stirring under $N_2$, the system was refluxed for 24 hours. The solution was extracted with dichloromethane, and then dried with $MgSO_4$. The resulting crude product was purified by column chromatography using silica gel (2.51 g, 90%). $^1H$ NMR (400 MHz, Chloroform-*d*) δ 10.08 (s, 3H), 7.98 (dq, *J* = 8.4, 2.1 Hz, 6H), 7.81-7.76 (m, 6H), 7.66-7.60 (m, 6H), 7.33-7.29 (m, 6H). $^{13}C$ NMR (101 MHz, $CDCl_3$) δ 191.81, 147.48, 146.32, 134.99, 134.47, 130.39, 128.40, 127.11, 124.66. $^1H$ NMR and $^{13}C$

NMR spectrum was shown in Fig S5 and Fig S6.


Fig. S5. $^{1}$H NMR spectrum of **NTBCA**.

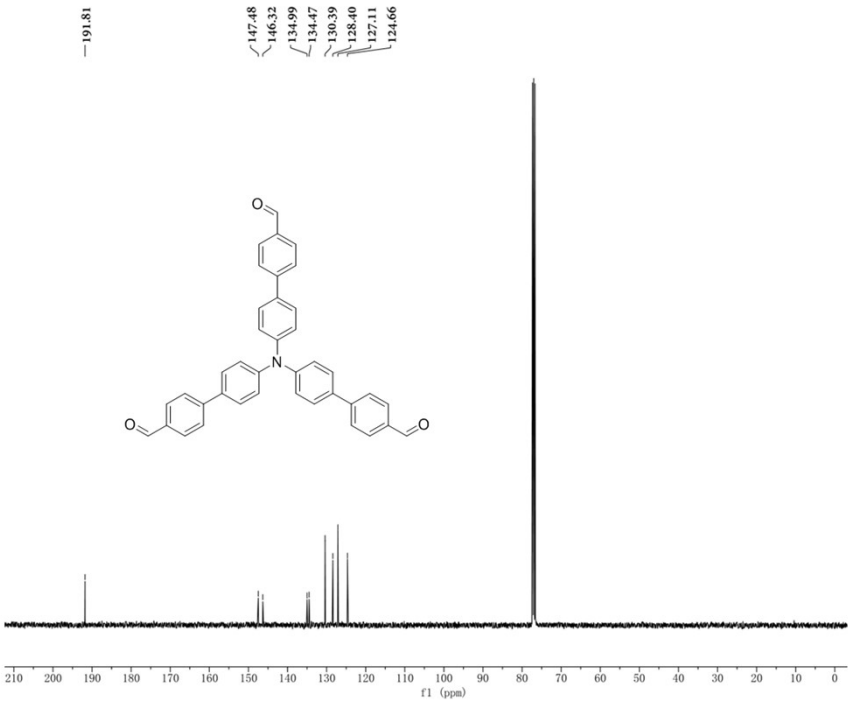


Fig. S6. $^{13}$C NMR spectrum of **NTBCA**.

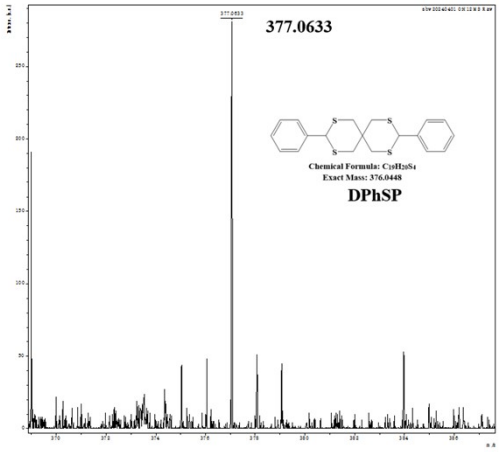


Fig. S7. HR-MS of **DPhSP**.

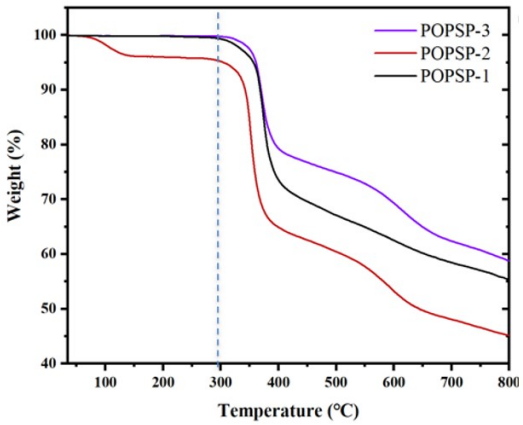


Fig. S8. TGA of POPSPs.

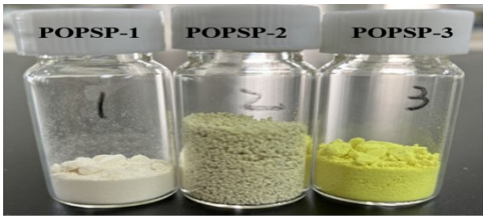


Fig. S9. Digital images of POPSPs.

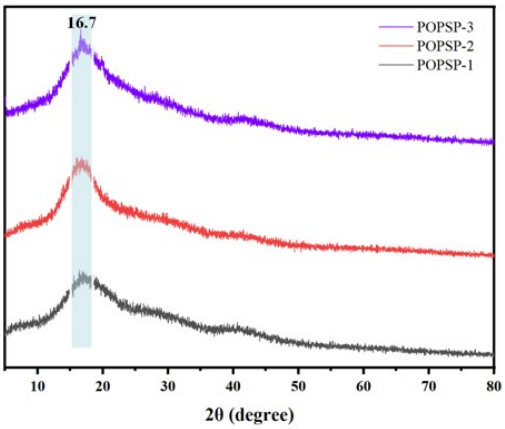


Fig. S10. PXRD of POPSPs.

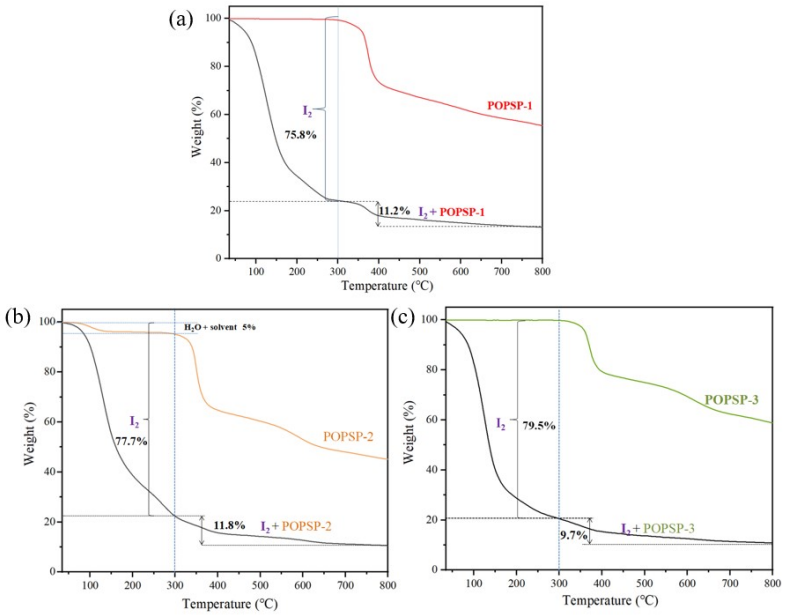


Fig. S11. TGA of $I_2$@POPSPs.

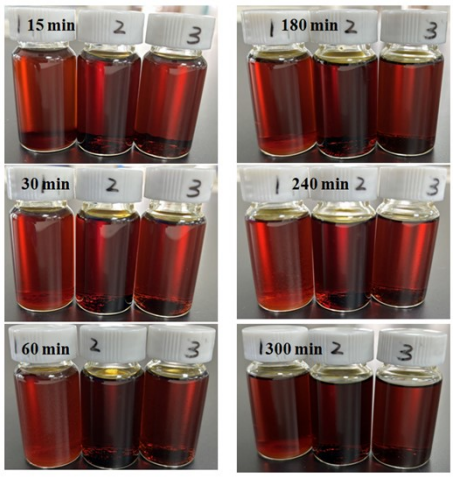


Fig. S12. $I_2$@POPSPs were immersed in EtOH.

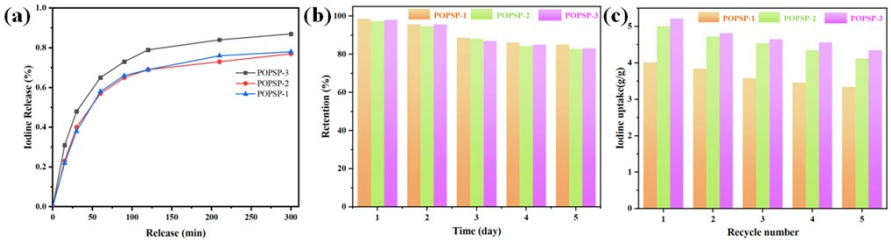


Fig. S13. (a) Iodine release curves of $I_2$@POPSPs. (b) Iodine retention of $I_2$@POPSPs upon exposure to air at 25 °C and 1 bar. (c) Recyclability of POPSPs for adsorbing iodine.

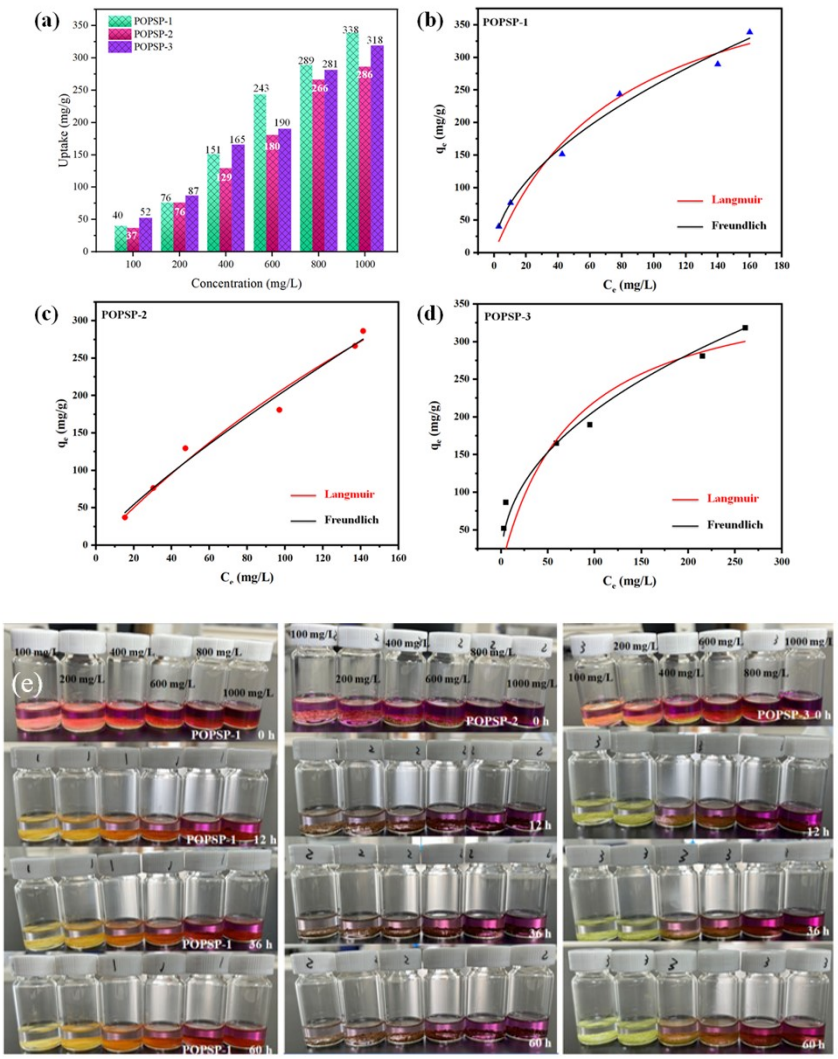


Fig. S14. (a) Iodine uptake performance of POPSP-1, POPSP-2, and POPSP-3 in *n*-hexane solution. The Langmuir adsorption model and Freundlich adsorption model for POPSP-1 (b), POPSP-2 (c), and POPSP-3 (d). (e) Three polymers were immersed in iodine/hexane solutions of different concentrations.

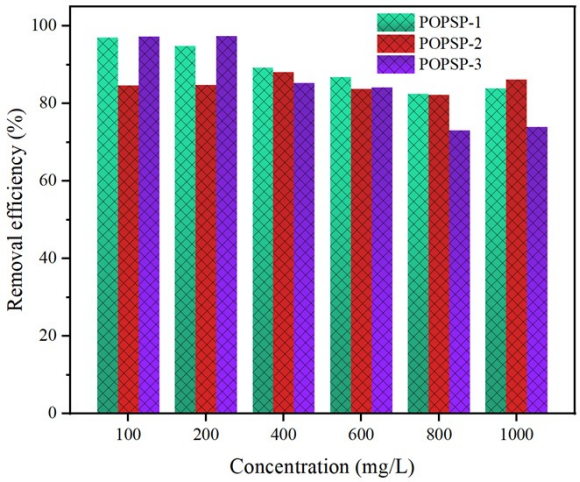


Fig. S15. The iodine removal efficiency of POPSPs in solutions.

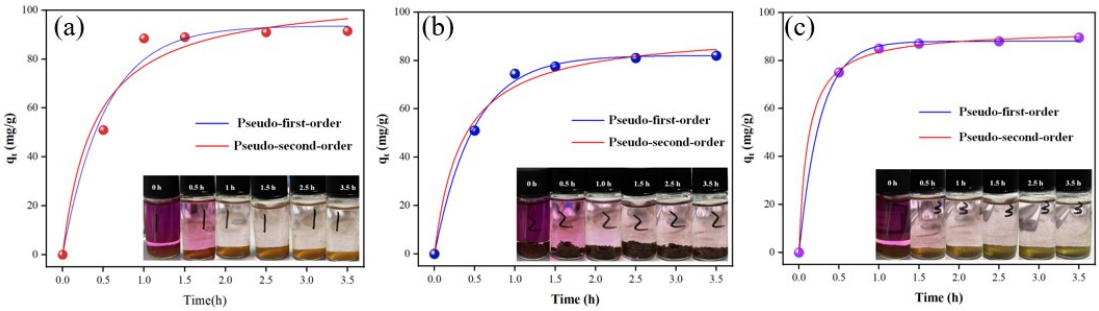


Fig. S16. Kinetic studies of iodine adsorption, pseudo-first-order, and pseudo-second-order linear fitting plots for iodine capture by POPSP-1 (a), POPSP-2 (b), and POPSP-3 (c) in cyclohexane solutions (200 mg/L). The inserts in the figure show the color change over time when POPSP-1 (a), POPSP-2 (b), and POPSP-3 (c) were soaked in the n-hexane solution of $I_2$.

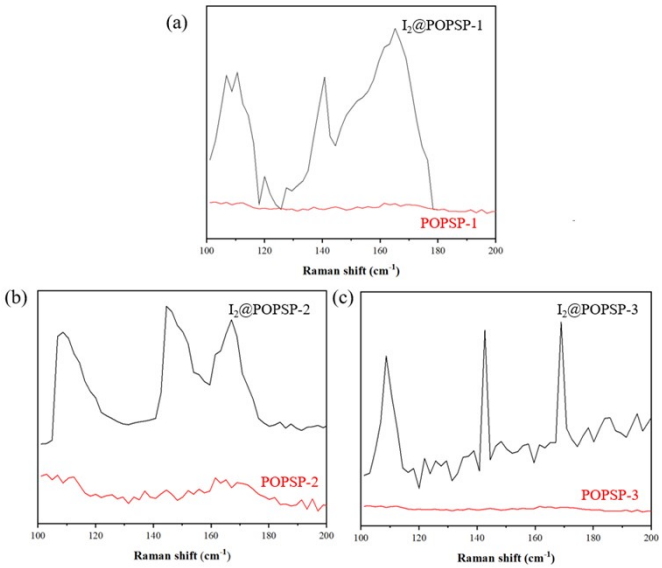


Fig. S17. Raman of POPSPs and $I_2$@ POPSPs.

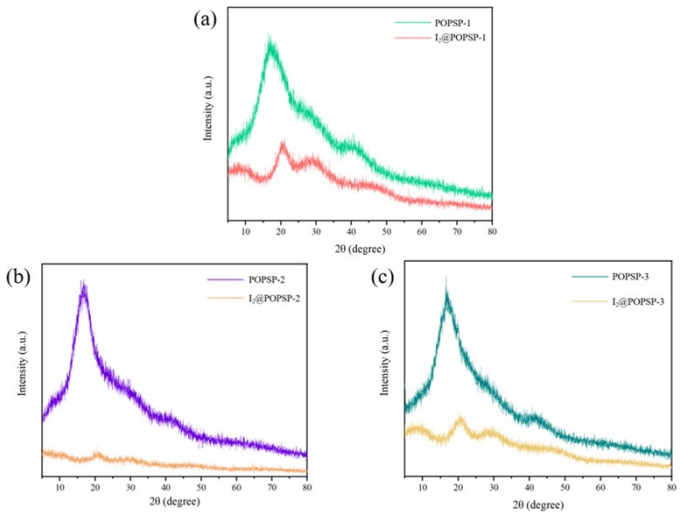


Fig. S18. PXRD plot of POPSPs and $I_2$@POPSPs.

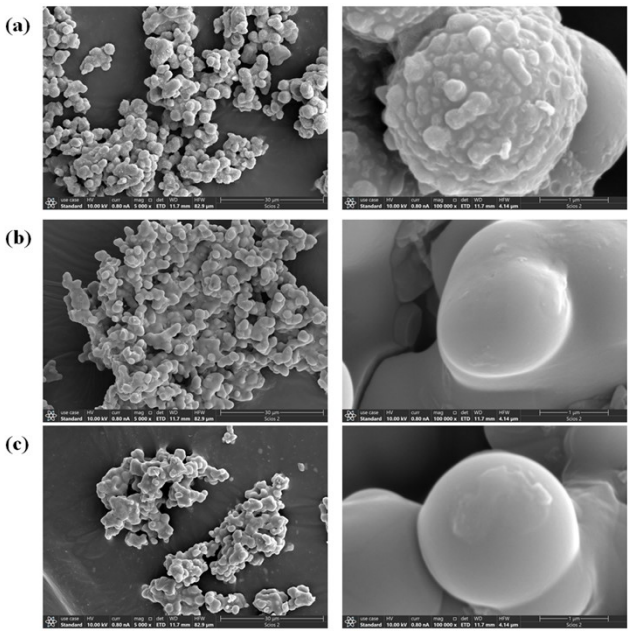


Fig. S19. SEM images of (a) $I_2$@POPSP-1, (b) $I_2$@POPSP-2, and (c) $I_2$@POPSP-3.

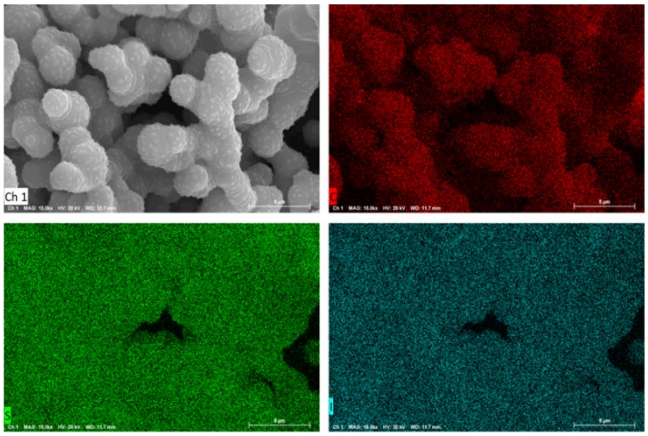


Fig. S20. EDX elemental mapping images of $I_2$@POPSP-1.

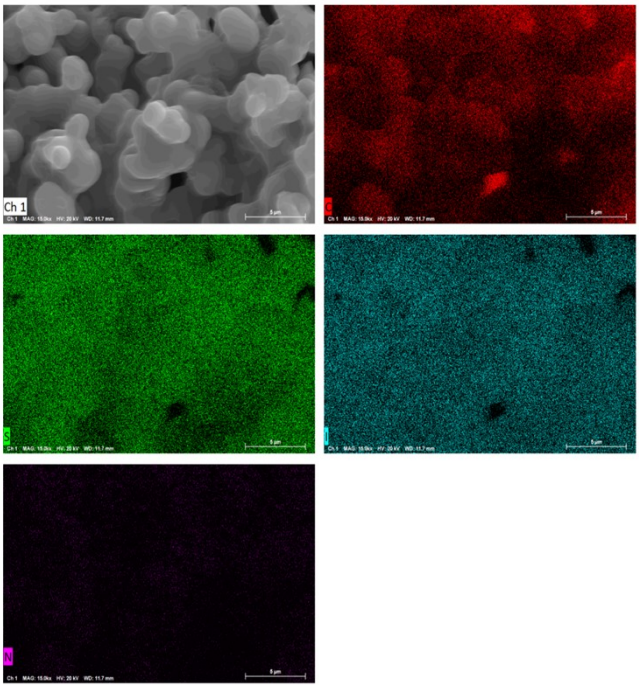


Fig. S21. EDX elemental mapping images of $I_2$@POPSP-2.

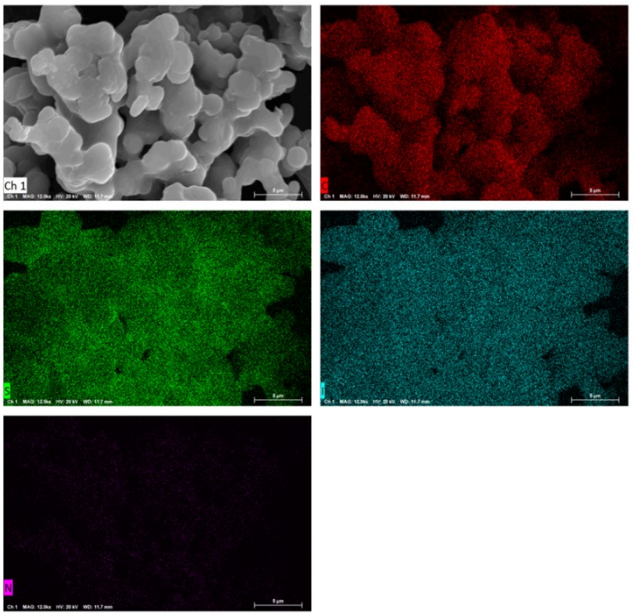


Fig. S22. EDX elemental mapping images of $I_2$@POPSP-3.

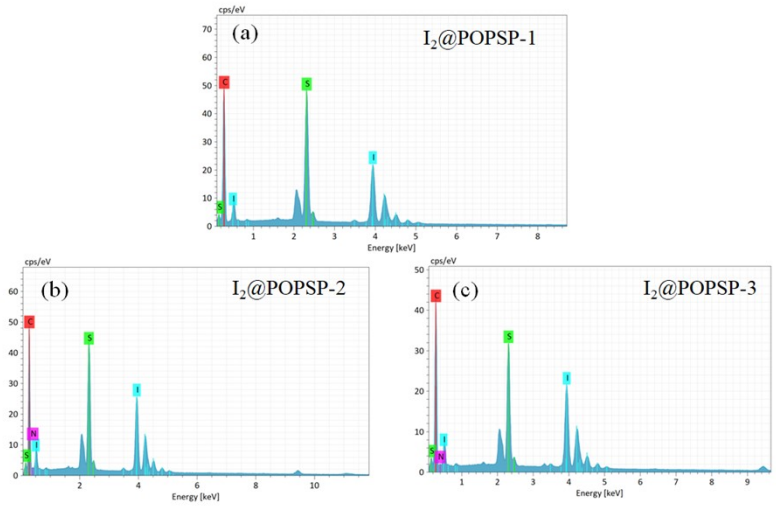


Fig. S23. EDX spectra of (a) $I_2$@POPSP-1, (b) $I_2$@POPSP-2, and (c) $I_2$@POPSP-3.

**Iodine vapor adsorption experimental procedure.**

A gravimetric measurement was conducted to investigate the capture of iodine vapor. The synthesized powders were placed in a 2 mL glass bottle, then a 20 mL sealed bottle was used to hold the superfluous iodine and the glass bottle at a temperature of 75 °C and an ambient pressurized environment. The polymers had been adsorbed with iodine in a period time of adsorption, was cooled to 25 ℃ and subsequently weighed. The polymer's iodine uptake capacity was determined using the Equation (1) as follows:

$$Iodine\ uptake\ capacity\ (wt\%) = \frac{W_2 - W_1}{W_1} \times 100\% \quad (1)$$

The $W_2$ and $W_1$ values of PIPCOP were used to denote their weight before and after iodine capture, respectively.

**Experiment procedures of iodine adsorption in n-hexane.**

The adsorption experiment of POPSPs in solution was carried out in n-hexane solution of iodine. A series of iodine-n-hexane solutions (20 mL) with different concentrations (100 mg/L, 200 mg/L, 400 mg/L, 600 mg/L, 800 mg/L and 1000 mg/L, respectively) were first prepared. Then, POPSPs was dispersed in the solution for a given time at room temperature. The mixture was filtered with 0.22μm Millipore cellulose membrane before UV-visible absorption spectrum analysis. The saturated adsorption amount of iodine in the n-hexane solutions was measurement after 48

hours' adsorption. The iodine uptake capacity of CMPs in solution was evaluated according to the following equation:

$$R = \frac{(C_0 - C_t)}{C_o} \quad (2)$$

$$Q_t = \frac{(C_0 - C_t)}{W} * V \quad (3)$$

where $R$ is the iodine removal rate of POPSPs in n-hexane solution and $Q_t$ is the adsorption value of iodine in the solution at a given time. $C_t$ represents the iodine concentration of the supernatant after adsorption of iodine, $C_0$ represents the iodine concentration of the initial supernatant, $V$ represents the volume of n-hexane solution, and $W$ represents the mass of CMPs.

**Kinetic Equations for Adsorption Study.**

The pseudo-first-order kinetics equation is given as follows:

$$\ln(q_e - q_t) = lnq_e - k_1 t \quad (4)$$

where $q_t$ and $q_e$ are the adsorption capacity (mg/g) at a given time $t$ (min) and at equilibrium, respectively, and $k_1$ is the rate constant for the pseudo-first-order adsorption ($min^{-1}$).

The pseudo-second-order kinetics equation is given as follows:

$$dq_t/dt = k_2(q_e - q_t)^2 \quad (5)$$

$$t/q_t = \frac{1}{k_2 q_e^{\,2}} + {}^{t}/_{q_e} \quad (6)$$

where $q_t$ is the adsorption capacity (mg/g) at given time $t$ (min) and $q_e$ is the adsorption capacity at equilibrium (mg/g). $k_2$ is the rate constant of pseudo-second-order adsorption ($g \cdot mg \cdot min^{-1}$).

Langmuir and Freundlich isotherm models were employed to evaluate adsorption isotherm according to Eq. (7) and Eq. (8), respectively.

$${C_e}/{q_e} = {1}/{(q_m k_L)} + {C_e}/{q_m} \quad (7)$$

$$lnq_e = lnk_F + {1}/{n} lnC_e \quad (8)$$

where, $q_e$ (mg/g) is the equilibrium adsorption capacity, $C_e$ (mg/L) is the equilibrium concentration of iodine, $q_m$ (mg/g) is the maximum adsorption capacity, $k_L$ is the Langmuir equilibrium adsorption constant, $k_F$ and n are Freundlich constants

related to the sorption capacity and sorption intensity, respectively.

Table S1. Summary of iodine vapor uptake abilities by sulfur-containing porous organic polymers

| Adsorbents | Temperature (°C) | Total pore volumes ($cm^3\ g^{-1}$) | $S_{BET}$ ($m^2\ g^{-1}$) | Iodine uptake (wt%) | Ref. |
|---|---|---|---|---|---|
| POPSP-1 | 75 | 0.011 | 3.59 | 4.13 | This work |
| POPSP-2 | 75 | 0.012 | 4.50 | 5.25 | This work |
| POPSP-3 | 75 | 0.007 | 2.31 | 5.65 | This work |
| PCS-DPBS | 70 | 0.150 | 245 | 2.81 | S5 |
| BTT-TAPT-COF | 78 | 0.56 | 864 | 2.76 | 28 |
| PZHCP-1:4 | 75 | 0.24 | 209 | 3.33 | S6 |
| HCPs-S | 75 | 0.46 | 167 | 1.79 | S7 |
| SHCMP-1 | 78 | 0.45 | 75 | 5.90 | 24 |
| SHCMP-2 | 78 | 0.36 | 86 | 4.95 | 24 |
| P-TzTz | 78 | - | 137 | 3.26 | S8 |
| PTZ-TPC-MA | 75 | - | 131 | 1.98 | S9 |
| JUC-560 | 75 | 1.11 | 1815 | 5.20 | 30 |
| JUC-561 | 75 | 1.92 | 2359 | 8.19 | 30 |
| TTDA | 77 | 0.88 | 1536 | 3.34 | 32 |
| HTDA | 77 | 1.06 | 1798 | 4.38 | 32 |
| COF-S1 | 75 | 1.67 | 2133 | 7.74 | 33 |
| COF-S2 | 75 | 1.18 | 1430 | 7.13 | 33 |
| SCMP-1 | 80 | 0.23 | 172 | 1.88 | S10 |
| SCMP-2 | 80 | 1.50 | 308 | 2.22 | S10 |
| TTDP-1 | 75 | - | 12 | 5.36 | 45 |
| TTDP-2 | 75 | - | 7.4 | 4.70 | 45 |
| TTDP-3 | 75 | - | 13.2 | 4.25 | 45 |
| PA-TT | 75 | 0.112 | 48.6 | 5.1 | 31 |
| PB-TT | 75 | 0.986 | 1305 | 5.97 | 31 |

Table S2 Kinetic parameters for the iodine capture by POPSPs.

| | Pseudo-first-order kinetic model | | | Pseudo-second-order kinetic model | | |
|---|---|---|---|---|---|---|
| | $q_e$ (wt%) | $k_1$ (1/h) | $R^2$ | $q_e$ (wt%) | $K_2$ [g/(g·h)] | $R^2$ |
| **POPSP-1** | 426 | 0.10861 | 0.9978 | 561 | 0.01711 | 0.9992 |
| **POPSP-2** | 542 | 0.1363 | 0.9959 | 686 | 0.0189 | 0.9863 |
| **POPSP-3** | 591 | 0.11077 | 0.9982 | 779 | 0.0125 | 0.9946 |

Table S3. The kinetic parameters corresponding to the capture of iodine/hexane solutions (200 mg/L) by POPSPs.

| | **Pseudo-first-order** | | | **Pseudo-second-order** | | |
|---|---|---|---|---|---|---|
| | $q_e$ (wt%) | $k_1$ (1/h) | $R^2$ | $q_e$ (wt%) | $K_2$ [g/(g·h)] | $R^2$ |
| POPSP-1 | 93.6 | 1.91 | 0.981 | 107.3 | 0.0238 | 0.962 |
| POPSP-2 | 82.1 | 2.05 | 0.997 | 92.8 | 0.0314 | 0.989 |
| POPSP-3 | 88.0 | 3.76 | 0.99938 | 92.8 | 0.0964 | 0.99930 |

**References**

S1 Y. Wan, O. Mitkin, L. Barnhurst, A. Kurchan and A. kutateladze, *Org. Lett.* **2000**, 2, 24, 3817–3819.

S2 S. Tseng and T. Yang, Tetrahedron: *Asymmetry* **2004**, 15, 3375–3380.

S3 Y. Lan, X. Han, M. Tong, H. Huang, Q. Yang, D. Liu, X. Zhao and C. Zhong, *Nat. Commun.* **2018**, 9, 5274.

S4 C. Zhang, Y. Zhang, Z. Zhang, X. Wu, Q. Yu and Y. Liu, *Chem. Commun.* **2019**, 55, 8138-8141.

S5 Z. Wang, R. Kunthom, S. V. Kostjuk and H. Liu, Eur. *Polym. J.* **2023**, 192, 112072.

S6 C. Yan, Y. Wu, H. Lu, H. Liu, G. Yi, M. Li, X. Cai, S. Gao and Z. Yang, *Micropor. Mesopor. Mat.* **2022**, 343, 112157.

S7 H. Ma, Q. Zhang, G. Cheng, Z. Wang, Q. Zong, B. Tan and C. Zhang, *Acs Appl. Polym. Mater.* **2021**, 3, 209-215.

S8 X. Pan, C. Ding, Z. Zhang, H. Ke and G. Cheng, *Micropor. Mesopor. Mat.* **2020**, 300, 110161.

S9 N. Qiu, H. Wang, R. Tang, Y. Yang, X. Kong, Z. Hu, F. Zhong and H. Tan, *Micropor. Mesopor. Mat.* **2024**, 363, 112833.

S10 X. Qian, Z. Q. Zhu, H. X. Sun, F. Ren, P. Mu, W. Liang, L. Chen and A. Li, *Acs Appl. Mater. Interfaces* **2016**, 8, 21063-21069.